Lisfranc Joint Ligamentous Complex: MRI With Anatomic Correlation in Cadavers

Miguel Castro[1]
Lina Melão[1,2]
Clarissa Canella[2]
Marcio Weber[2]
Pedro Negrão[3]
Debra Trudell[2]
Donald Resnick[2]

OBJECTIVE. The aim of our study was to clarify the ligamentous anatomy of the Lisfranc joint complex and show the diagnostic capability of MRI in the assessment of the Lisfranc joint complex with detailed anatomic correlation in cadavers.

MATERIALS AND METHODS. Ten fresh cadaveric feet were studied with high-spatial-resolution MRI before and after the intraarticular injection of a gadopentetate dimeglumine solution. MR images were evaluated by two readers in consensus, with emphasis on the visibility of the ligamentous structures and their appearance. Readers also measured the dimensions (length, width, and thickness) of the Lisfranc ligament and of the first plantar tarsometatarsal ligament, or plantar Lisfranc ligament. For anatomic analysis, nine cadaveric specimens were sectioned in 3-mm-thick slices in the same planes used during MRI. One additional foot specimen was used for dissection.

RESULTS. In all 10 cadaveric specimens we were able to identify and characterize with MRI the different ligamentous elements that contribute to the overall stability of the Lisfranc joint complex.

CONCLUSION. By clearly defining the normal ligaments that contribute to the stability of the Lisfranc joint, MRI allows a more precise and correct diagnosis of the origin of the Lisfranc joint instability, perhaps permitting a more specific surgical management. MRI also allows a better understanding of the normal imaging anatomy of the different ligamentous components of the Lisfranc joint, mainly of the Lisfranc and plantar Lisfranc ligaments.

Keywords: ligamentous anatomy, Lisfranc joint, Lisfranc ligament, MRI, plantar Lisfranc ligament

DOI:10.2214/AJR.10.4674

Received March 25, 2010; accepted without revision April 26, 2010.

[1]Faculdade de Medicina da Universidade do Porto, Hospital São João, Alameda Professor Hernâni Monteiro, 4200-451 Porto, Portugal. Address correspondence to Miguel Castro (miguelhcastro@gmail.com).

[2]Radiology Department, University of California, San Diego, VA San Diego Healthcare System, San Diego, CA.

[3]Orthopaedic Department, Hospital Geral de Santo António, 4099-001 Porto, Portugal.

WEB
This is a Web exclusive article.

AJR 2010; 195:W447–W455

0361–803X/10/1956–W447

Low-energy injuries to the tarsometatarsal (TMT) joints, also known as Lisfranc's articulation, are frequently acquired during sports and recreational activities, resulting in midfoot sprains. Unlike high-energy injuries, these low-energy midfoot injuries are challenging to manage because of the difficulty in identifying the specific structures that have been injured [1–6].

The Lisfranc joint is a complex polyarticular system with an intricate anatomic configuration of skeletal and nonskeletal elements, such that the authors prefer to use the term "Lisfranc joint complex" [2, 7–9]. The skeletal elements are composed of the tarsometatarsal, intertarsal, and intermetatarsal articular surfaces. The nonskeletal elements comprise the articular capsules, the various ligaments, the prolongations of the long plantar ligament (inferior calcaneocuboid ligament), and the tendons and expansions of the tibialis posterior, tibialis anterior, and peroneus longus, which all function to maintain the stability of the TMT joints [7, 9].

Even though recent advances in MRI techniques have improved the specificity for the diagnosis of injuries to the different ligaments of the Lisfranc complex, the distinction between the Lisfranc ligament and the nearby plantar ligaments has not always been clearly made in the past. Several imaging studies have been published that define the role of MRI in the diagnosis of ligamentous injury of the foot and ankle [1, 6, 10–15]. Only one of these defined the Lisfranc and the plantar ligaments as separate structures [14].

The current study was undertaken to gain a more detailed knowledge of the imaging anatomy of the Lisfranc articulation, because such knowledge is a precondition to a more precise and reliable diagnosis of its injuries.

Materials and Methods

Cadaveric and Specimen Preparation

Ten foot specimens (four right and six left), transected approximately 8–10 cm proximal to the

ankle joint, were removed from 10 fresh cadavers (six men and four women; age at death, 64–89 years; mean age at death, 77.5 years) and were immediately deep frozen at –40°C (Forma BioFreezer, Forma Scientific). All specimens were allowed to thaw for at least 24 hours at room temperature before TMT arthrography and MRI.

MRI

All the specimens were examined with MRI by using a 1.5 T machine (Signa, GE Healthcare) placed in neutral position in a standard foot coil. Proton density–weighted MR images (TR/TE 3,000/minimum full) were obtained in the axial, sagittal, and coronal planes, with a slice thickness of 1.5 mm, interslice gap of 0.5 mm, a matrix size of 320 × 224, a field of view of 10 cm, with two excitations and a bandwidth of 22 MHz. An additional transverse oblique plane, parallel to the distal portion of the peroneus longus tendon, was also acquired with the same parameters.

MR Arthrography

Three intraarticular injections were performed with a 22-gauge needle, through the dorsal and dorsolateral skin of the foot, at the level of the TMT, with fluoroscopic guidance. Each compartment (i.e., medial, central, and lateral TMT joints) was filled with approximately 3–5 mL of a contrast solution consisting of 1 mL of gadopentate dimeglumine (Magnevist, Bayer Healthcare) diluted in 250 mL of saline solution, 0.5 mL of iohexol, and 0.5 mL of a mixture of gelatin. Subsequently, MR images were obtained by using the same techniques and positions as previously outlined, with the addition in each plane of a proton density–weighted sequence with selective fat saturation.

Macroscopic Anatomy

After imaging, all 10 specimens were deep frozen again. Nine were cut with a band saw into 2- to 3-mm-thick sections, two in each of the standard planes (axial, coronal, and sagittal) and three in the transverse oblique plane. The anatomic sections were cleaned with running water for macroscopic inspection. Each slice was digitally photographed, and correlation with MR images was performed. One foot was dissected by an orthopedic surgeon to correlate the gross anatomy with the imaging findings.

MR Image Analysis

Qualitative evaluation—MR images were assessed for the evaluation of the visibility of the ligamentous structures in the Lisfranc joint complex and their signal intensity characteristics by the consensus of two radiologists with 2 and 3 years of experience in musculoskeletal imaging. For each of the ligaments, the following features were analyzed: visibility in each imaging plane (highly visible, visible, difficult to visualize, and not visible), appearance (homogeneous, striated/heterogeneous), configuration (one band, two or more bands, and shape), and signal intensity on proton density–weighted MR images (low or intermediate signal compared with the low signal intensity of the normal tendons).

Quantitative evaluation—The length (measuring the posterolateral border) and width (at the midportion) of the Lisfranc ligament and of the two bands of the first plantar tarsometatarsal ligament were measured on axial or transverse oblique MR images that best showed the entire ligament. The thickness of these same ligaments was measured on coronal MR images, for the Lisfranc ligament at its midpoint and for the first plantar tarsometatarsal ligament, near its proximal insertion on the medial cuneiform, before its bifurcation. The measurements were made on the MR images by using a PACS workstation and recorded separately by two of the authors.

Statistical Analysis

Software (SPSS 13.0, SPSS, Inc.) for Microsoft Windows was used for statistical analysis. The measurements obtained in men and women were compared using the Student's *t* test. To analyze the associations between ligament length, thickness, and width with variables such as the patient's age at death and gender, we calculated Pearson's correlation coefficients. A p value of < 0.05 was considered to indicate statistical significance.

Results

The following abbreviations are used: TMT = tarsometatarsal; C1 = medial cuneiform; C2 = intermediate cuneiform; C3 = lateral cuneiform; Cu = Cuboid; M1, M2, M3, M4, and M5 for each of the corresponding metatarsal bones. The articulations are referenced using a hyphen between the articulating bones; for example, the abbreviation for the second tarsometatarsal joint is C2-M2.

Capsules

The Lisfranc joint complex has three separate articular capsules, creating three distinct

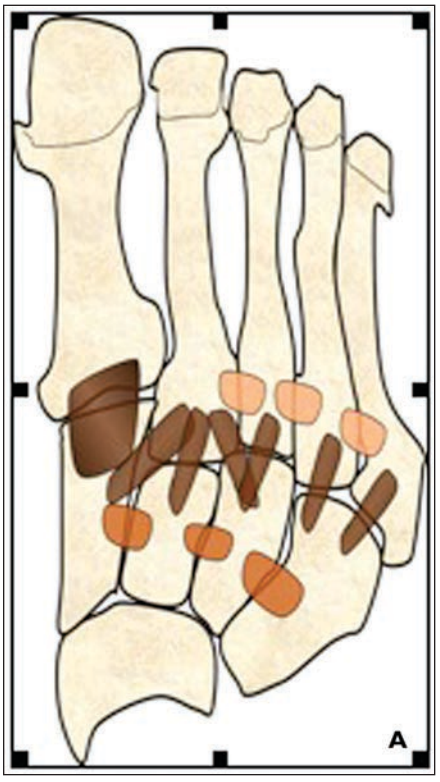

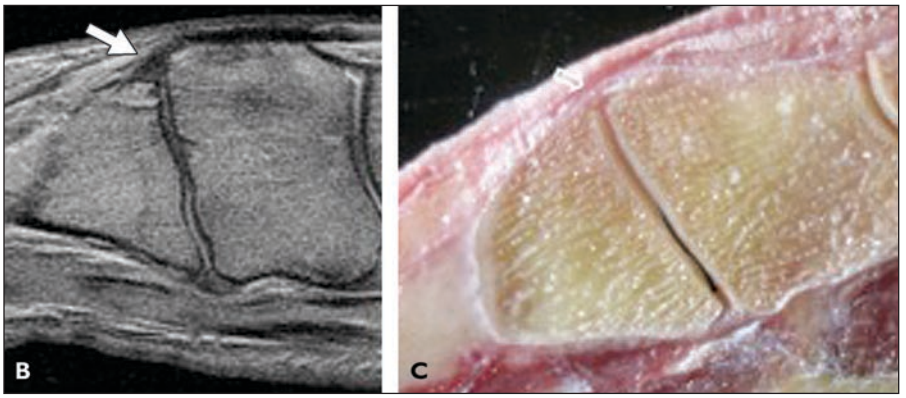

Fig. 1—Dorsal ligaments of Lisfranc joint complex.
A, Schematic representation of dorsal ligaments (*brown*) of Lisfranc joint complex. Dorsal intertarsal (*orange*) and intermetatarsal (*peach*) ligaments are also represented.
B and **C**, Sagittal proton density MR image after intraarticular injection of gadolinium solution (**B**) and photograph of corresponding gross anatomic section (**C**) in cadaveric specimen show short and flat dorsal tarsometatarsal ligament between C1 and M1 (*arrows*). Note homogeneous low signal intensity at MR image.

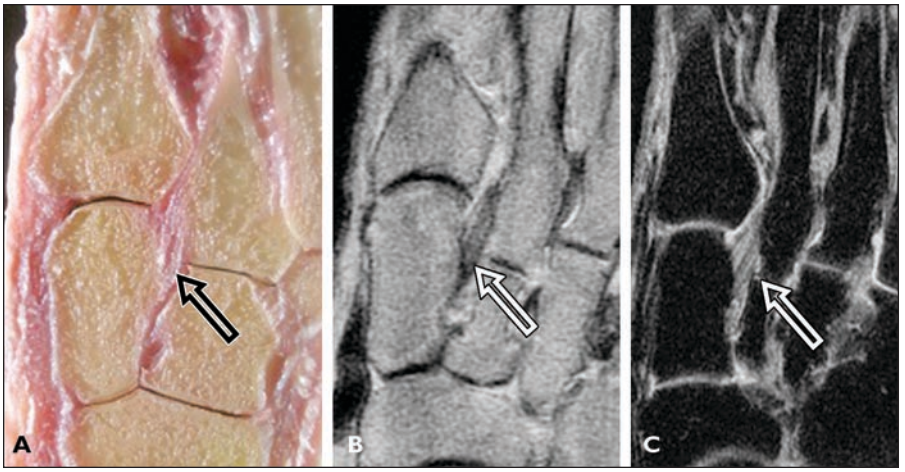

Fig. 2—Lisfranc ligament.
A–C, Photographs of gross anatomic section (**A**) and transverse oblique proton density images after intraarticular injection of gadolinium solution, without (**B**) and with (**C**) fat saturation, show Lisfranc ligament (*arrows*) extending from lateral surface of C1 to medial aspect of M2. Note striated appearance and intermediate signal intensity in MR images.

TABLE 1: Dimensions of the Lisfranc Ligament in 10 Cadaveric Feet on MRI

	Length (mm)	Width (mm)	Thickness[a] (mm)
Lisfranc ligament	9.17 ± 1.5 (6.6–10.95)	5.21 ± 1.28 (3.75–7.55)	6.9 ± 1.28 (5–9.1)

Note—Data are mean ± SD (range).
[a]In the two cases in which the Lisfranc ligament had two bands, the thickness was determined by measuring the two bands together.

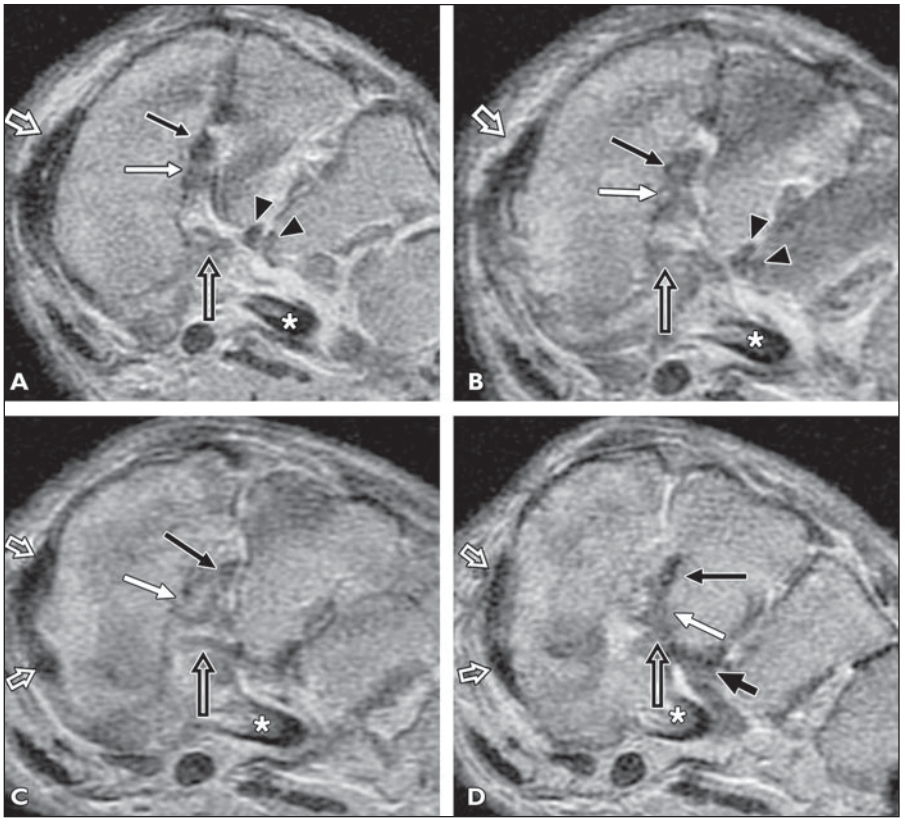

articular compartments: medial, central, and lateral. This was confirmed by arthrography in all 10 specimens, which showed the existence of three different synovial systems lacking communication with one another.

The medial compartment comprised only the C1-M1 articulation and did not communicate with other articulations. The central compartment was formed by various joints, which included C2-M2, C3-M3, C1-C2, C2-C3, M2-M3, C3-M2, and C3-M4. The lateral compartment contained the Cu-M4/M5 and M4-M5 articulations and did not communicate with the central compartment.

In eight of the 10 foot specimens there was unequivocal contact between the central compartment and the cuneonavicular joint, by way of the intercuneiform articulations (C1-C2 and C2-C3); in the other two specimens, this was not well shown, probably because of an insufficient volume of contrast agent.

TMT Ligaments

Dorsal TMT ligaments—Seven dorsal ligaments are included in the Lisfranc joint complex [7, 8] (Fig. 1). In all 10 specimens they were all short, flat, striplike bands, consistently homogeneous with low-signal intensity and formed only by one band. They were visible in the coronal and the sagittal planes but not seen on the axial or transverse oblique MR images.

Interosseous TMT ligaments—The Lisfranc ligament is the medial (first) interosseous ligament, C1-M2, and the largest of the three interosseous ligaments. It appears as an oblique ligament that arises from the lateral surface of C1, in front of the medial insertion of the intercuneiform ligament (Fig. 2). It extends distally, laterally, and slightly downward, inserting on the lower half of the medial aspect of M2 (Table 1).

In all specimens, the Lisfranc ligament was highly visible in the axial, transverse oblique, and coronal MR images but more

Fig. 3—Lisfranc ligament with two bands.
A–D, Four consecutive coronal proton density MR images at level of tarsometatarsal (TMT) joint are shown. In this specimen Lisfranc ligament has two bands, one superior (*solid black arrow*) and another inferior (*solid white arrow*), crossing from lateral aspect of C1 to medial surface of M2. Note "plantar Lisfranc" ligament (*open black arrow*) and its close proximity to Lisfranc ligament. Black arrowheads (**A** and **B**) correspond to distal extensions of posterior tibialis tendon. Open white arrows show anterior tibialis tendon, with its distal bifurcation in **C** and **D** to medial aspect of C1 and M1. Peroneus longus tendon (*asterisk*) crossing plantar tunnel to lateral aspect of base of M1 is also seen.

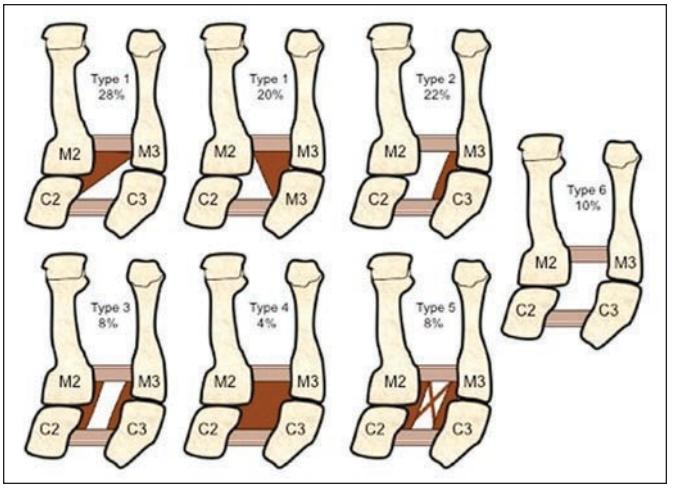

Fig. 4—Variations of second interosseous cuneometatarsal ligament. Beneath each type is incidence found in literature. In our sample we found 70% type 1 (50% with apex on C3 and 20% with apex on C2), 20% type 2, and 10% type 6.

difficult to see in the sagittal plane (described as "visible" in two specimens and "difficult to visualize" in eight specimens).

The Lisfranc ligament had either a striated (40%) or homogeneous (60%) appearance, as well as a low (50%) or intermediate (50%) signal intensity. In all cases in which it had a striated appearance, the ligament showed intermediate signal intensity (Fig. 2).

In two specimens, the Lisfranc ligament was formed by two bands, one superior and one inferior, better depicted on the coronal images (Fig. 3). On plantar aspect, the ability to discriminate it from the corresponding plantar Lisfranc ligament was only partially possible, because the two ligaments only had distinguishable borders along a portion of the contact area, mainly the proximal one.

There was no significant correlation between the thickness, length, width, and qualitative characteristics of this ligament and the age or sex of the specimens.

The second interosseous cuneometatarsal ligament (i.e., central, middle, or intermediate interosseous ligament), located between the cuneiforms (C2 and C3) and the metatarsals (M2 and M3), has a complex and quite variable ligamentous arrangement. Six arrangements for this ligament have been described [7, 8] (Fig. 4). We found one foot that did not show evidence of any ligamentous structure in this interspace (Fig. 5). Six specimens showed the most common configuration (type 1) in which the ligament forms a triangular, obliquely placed lamina or band, extending from one cuneiform to the corresponding and opposite metatarsals (Fig. 6). Of these, four had an origin on C3, and two on C2, anterior to the intercuneiform (C2-C3) ligament. It was difficult to visualize this ligamentous structure in three of the foot specimens, and only with analysis of the MR arthrographic images and different imaging planes was it possible to discern a very faint

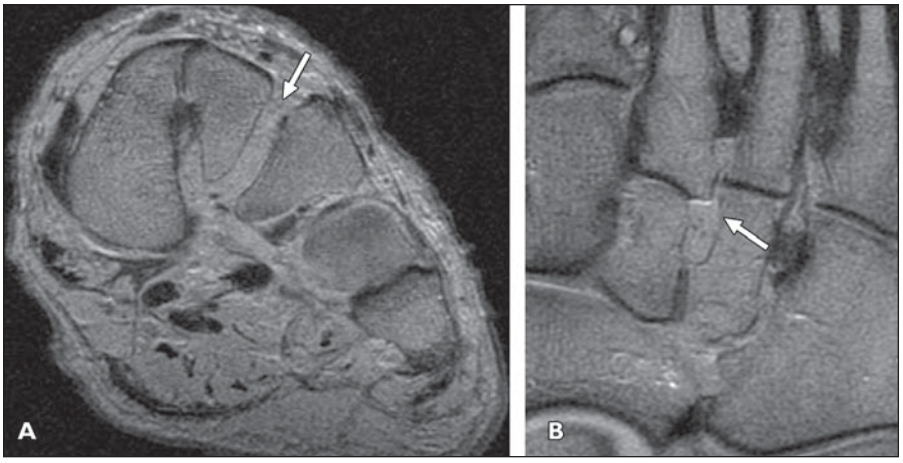

Fig. 5—Absent second interosseous cuneometatarsal ligament.
A and **B,** Coronal (**A**) and axial (**B**) proton density MR images after intraarticular injection of gadolinium solution showing absent ligamentous structure in second tarsometatarsal space (*white arrows*).

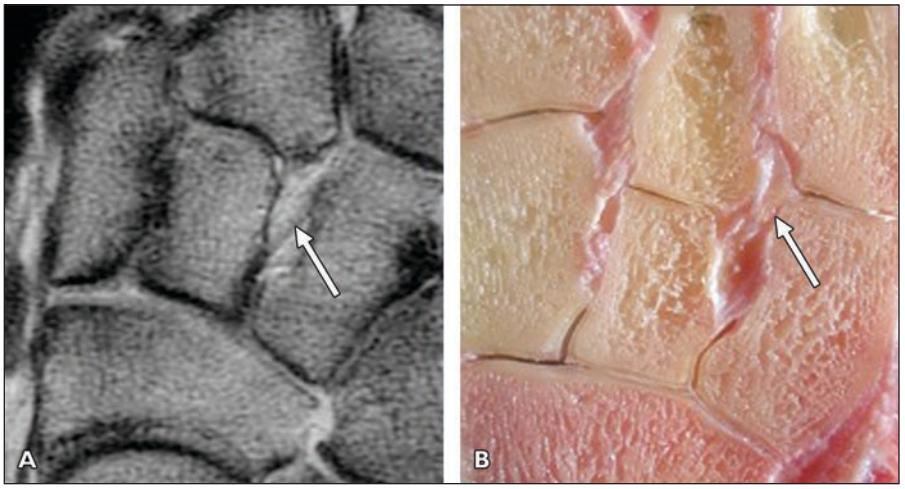

Fig. 6—Type 1 second interosseous cuneometatarsal ligament.
A and **B**, Axial proton density MR image after intraarticular injection of gadolinium solution (**A**) and photograph of corresponding gross anatomic section (**B**) in cadaveric specimen show type 1 second interosseous cuneometatarsal ligament (*arrows*) with apex of triangular lamina on C2.

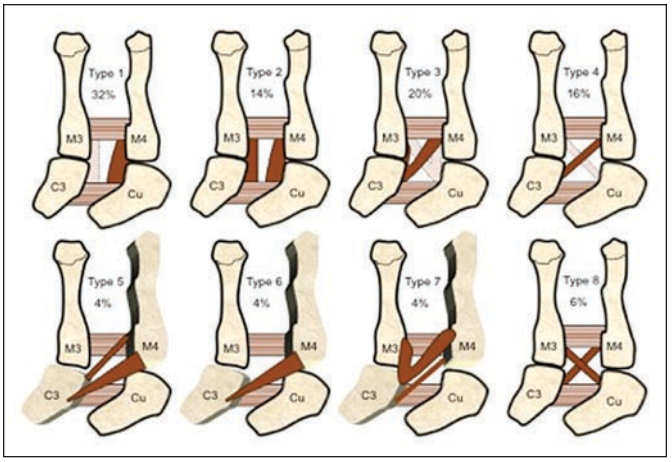

Fig. 7—Variations of third interosseous cuneometatarsal ligament. Beneath each type is incidence found in literature. In our sample we found 40% type 1, 10% type 2, 30% type 3, and 20% type 4.

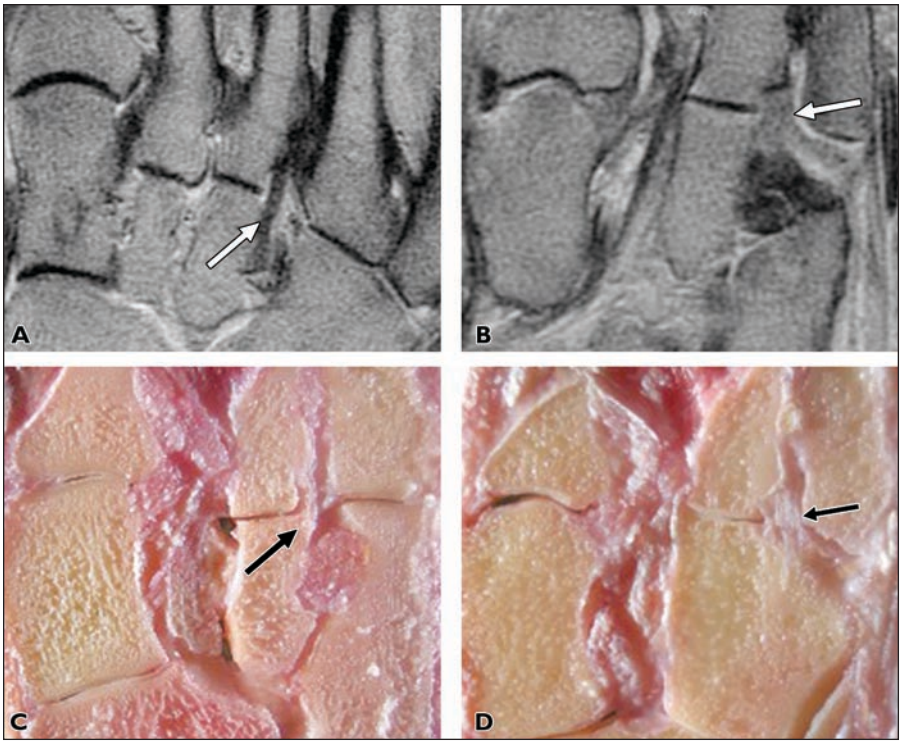

Fig. 8—Type 1 third interosseous cuneometatarsal ligament.
A–D, Transverse oblique (**A**) and axial (**B**) proton density MR images after injection of intraarticular gadolinium solution and corresponding anatomic sections (**C** and **D**) show two cases of type 1 third interosseous cuneometatarsal ligament (*arrows*) with single band connecting lateral aspects of C3 and M3.

ligament. Of these specimens, one revealed the most common pattern (type 1, C3-M2), and the other two showed a single band connecting the cuneiform and the metatarsal of the same ray (type 2), in one specimen from C3 to M3 and in the other from C2 to M2 (Fig. 4).

When present, the second interosseous ligament was always visible on the coronal MR images, but the best planes to appreciate its configuration were the axial and transverse oblique. In the proton density–weighted MR images, this interosseous ligament was heterogeneous with intermediate to low signal intensity.

The third or lateral interosseous ligament also has a variable morphology with at least eight types described [7, 8] (Fig. 7). In our sample, this interspace always revealed a ligamentous structure. Forty percent of the specimens showed a type 1 pattern, in which the ligament extended from the lateral aspect of the C3 to the base of the M3 (Fig. 8). A type 3 arrangement was found in 30% of the foot specimens. It consisted of a "V" arrangement that originated from the lateral aspect of C3 (20%) or from the medial side of the cuboid (10%) and inserted on M3 and M4. Twenty percent of the specimens displayed a type 4 design in which an oblique band extended from the medial aspect of cuboid to the base of M3. Finally, there was one specimen (10%) with a type 2 configuration that had two longitudinal bands present in each corresponding ray, i.e., C3-M3 and Cu-M4.

We were able to visualize the third interosseous ligament in the axial and transverse oblique planes and in the coronal planes. It showed homogeneous low signal intensity in nine specimens.

Plantar TMT Ligaments

The first plantar ligament, C1-M1, was a longitudinal and rectangular ligament, arising from the plantar aspect of C1, near the articular surface, extending slightly outward and distally to the lateral portion of M1 (Fig. 9). It showed a homogeneous low signal appearance in all specimens. It was highly visible on the axial, sagittal, and transverse oblique MR images.

The second plantar ligament, C1-M2,3, was designated the plantar Lisfranc ligament because of its position, orientation, and connection with the Lisfranc ligament. It arises from the inferolateral surface of C1, below the

Fig. 9—Schematic representation of plantar ligaments (*brown*) of Lisfranc joint complex. Plantar intertarsal (*orange*) and intermetatarsal (*peach*) ligaments are also represented.

Lisfranc ligament insertion, proximal and deep in relation to the insertion of the peroneus longus tendon. Then it takes an oblique course, oriented laterally and distally (Fig. 10). Proximally, it splits into a superficial component that inserts on the base of M3 and a deeper band that attaches at the base of M2, on its medial aspect (Fig. 11). This ligament was depicted in all foot specimens. In two cases, the different bands arose separately from C1, without the common insertion that is usually described (Fig. 12).

The M2 band was shorter than the M3 band, and the widths were very similar (Table 2).

Both components were always visualized in the coronal plane (50% highly visible and 50% visible) but were better evaluated and delineated in the axial and transverse oblique imaging planes (90% highly visible and 10% visible).

The plantar Lisfranc ligament consistently showed intermediate signal and a striated appearance.

We did not find any significant correlation between the dimensions, appearance, and signal intensity of this ligament and the age or sex of the specimens.

As noted already, no plantar ligaments between C2 and M2 were found [7, 8].

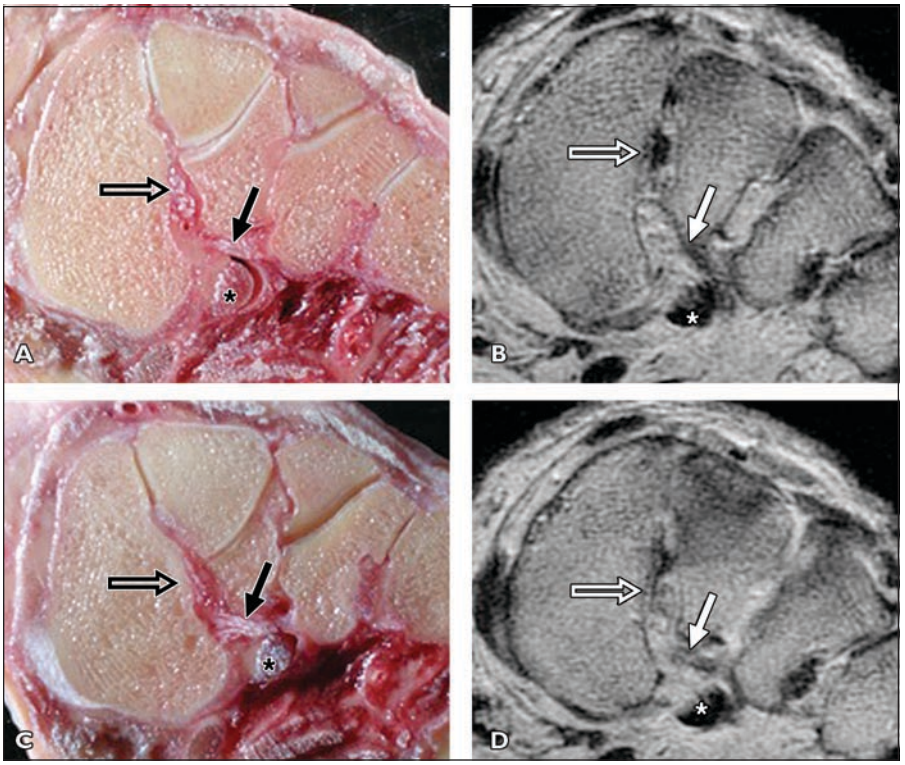

Fig. 10—Plantar Lisfranc ligament.
A–D, Consecutive coronal anatomic sections (**A** and **C**) and corresponding proton density MR images after injection of intraarticular gadolinium solution (**B** and **D**) show plantar Lisfranc ligament (*white and black arrows*) and Lisfranc ligament (*open arrows*). Peroneus longus tendon is also seen (*asterisk*).

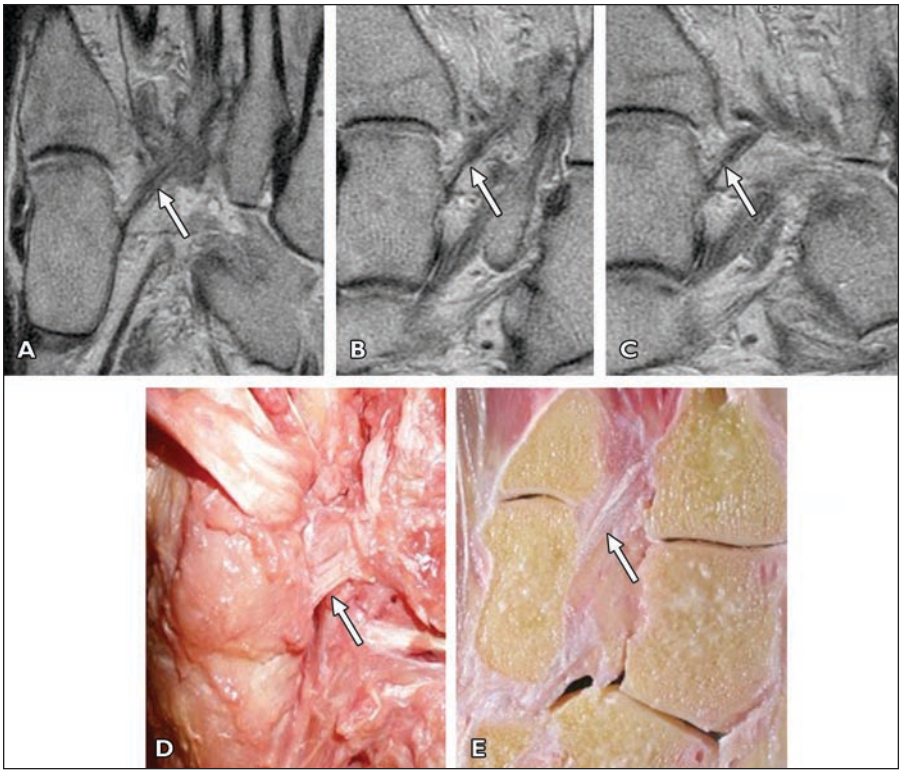

Fig. 11—Plantar Lisfranc ligament.
A–C, Consecutive axial proton density MR images after injection of intraarticular gadolinium solution show plantar Lisfranc ligament with its two bands: M3 band (*white arrow* in **A**) attaches to base of M3; and M2 band (*white arrows* in **B** and **C**) inserts on base of M2.
D, Dissected cadaveric foot from plantar view with peroneus longus tendon reflected upward shows plantar Lisfranc ligament (*white arrow*).
E, Corresponding anatomic axial section shows plantar Lisfranc ligament (*white arrow*).

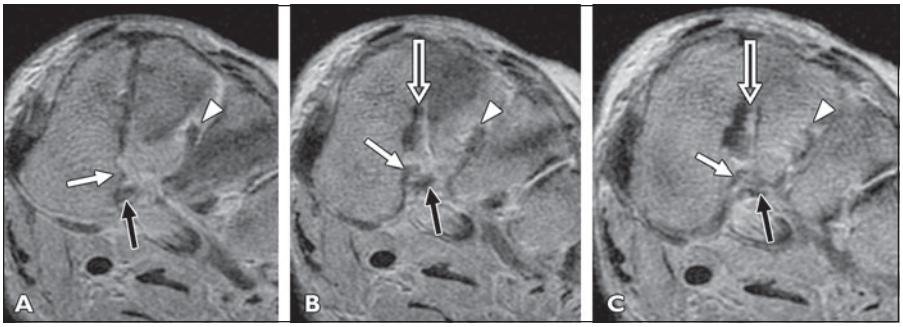

Fig. 12—Plantar Lisfranc ligament with two bands arising separately from C1.
A–C, Consecutive coronal proton density MR images after injection of intraarticular gadolinium solution show plantar Lisfranc ligament formed by two separate bands that did not show common C1 insertion. Instead, each band had its own insertion (M2 band of plantar Lisfranc ligament—*white arrows* and M3 band of plantar Lisfranc ligament—*black arrows*). Lisfranc ligament (*white open arrows*) and second interosseous cuneometatarsal ligament (*white arrowheads*) are also depicted.

TABLE 2: Dimensions of the Plantar Lisfranc Ligament in 10 Cadaveric Feet on MRI

	Length (mm)	Width (mm)	Thickness (mm)
Before bifurcation[a]			5.27 ± 0.83 (3.9–6.55)
M2 band	8.06 ± 1.13 (6.25–9.6)	3.97 ± 0.69 (3.1–5.15)	
M3 band	15.54 ± 1.61 (13.2–18)	3.99 ± 0.76 (3.1–5.35)	

Note—Data are mean ± SD (range).
[a]In the two cases in which the plantar Lisfranc ligament had two bands arising separately from C1, the thickness was determined by measuring the two bands together.

The third plantar ligament, C3-M3,4, is described as a bandlike ligament with an oblique orientation stretching from the inferolateral aspect of C3 to the bases of M3 and M4. We found it very difficult to separate completely this plantar ligament from the expansions of the long plantar ligament and the distal insertions of the tibialis posterior tendon, which have the same distal attachments and the same orientation as this plantar ligament.

The plantar ligaments between the cuboid and M4 and M5 were very thin, coursing longitudinally between the anterior–inferior aspect of the cuboid, immediately distal to the tunnel of the peroneus longus tendon, and the plantar and posterior aspect of the bases of M4 and M5. They were best seen in the sagittal plane.

Intermetatarsal and Intertarsal Ligaments

As already mentioned, the Lisfranc joint complex includes not only the TMT articular surfaces but also the intermetatarsal and anterior intertarsal surfaces. There are ligaments that reinforce and stabilize the articular capsules and skeletal elements, described in terms of dorsal, plantar, and interosseous ligaments.

We found two dorsal intercuneiform (C1-C2; C2-C3) (Fig. 13), one dorsal cuneocuboid, and three dorsal intermetatarsals (M2-M3, M3-M4, M4-M5) that were present in all specimens and best visualized in the coronal MR images (Fig. 1). They had a transverse or slightly oblique orientation and appeared as flat, rectangular, or bandlike ligaments with homogeneous low signal intensity.

The plantar intertarsal and intermetatarsal ligaments (Fig. 9) were more difficult to evaluate than the corresponding dorsal ligaments because of the complexity of the anatomy in the plantar aspect of the foot, but they were best depicted in the coronal plane. Only one plantar intercuneiform ligament was always present. It consistently connected the posterolateral aspect of C1 with the plantar crest of C2, except for one specimen in which the ligament extended directly from C1 to C3. We did not find any ligamentous structure between M1 and M2 on the dorsal or plantar aspect of the foot.

There were two interosseous ligaments that united the cuneiforms (C1-C2; C2-C3) and one that united C3 with the cuboid, completely filling their nonarticular surfaces. The latter was a short but very thick ligament consisting of two bands, one superior and the other inferior, in 80% of the specimens. Even when only one band was present, it showed a striated appearance and very low signal intensity (Fig. 14).

Finally, the three intermetatarsal interosseous ligaments uniting M2-M3-M4-M5 (a medial, a central, and a lateral), were visualized in the coronal, axial, and transverse oblique MR images (Fig. 14). As for the interosseous intertarsal ligaments, the lateral interosseous intermetatarsal ligament (M4-M5) was the most prominent, with a more oblique course than the other interosseous intermetatarsal ligaments.

Discussion

The aim of this study was to elucidate the precise anatomy of the Lisfranc joint ligamentous complex, in terms of MRI and MR arthrography, so that a more accurate diagnosis of injuries to this complex could be made. These injuries, although relatively uncommon, frequently occur in elite athletes, and disability and deformity may develop even when initial radiographs appear normal [2–6]. From an anatomical, mechanical, and functional point of view, the TMT, the intertarsal (intercuneiform and cuneocuboid), and the intermetatarsal articulations and ligaments belong to the Lisfranc joint complex; any disease process will involve them as a whole and not selectively [7, 8, 16, 17].

The relative importance of the different ligaments of the Lisfranc complex to the overall stability has been discussed in many previous reports [9, 11, 16, 17]. There is a general consensus that the most important ligaments are the ones coursing from the medial cuneiform to the second metatarsal base; these are also the ones most often disrupted in midfoot injuries [16, 17]. Secondary stabilizers of the joint are the insertions of the peroneus longus, tibialis anterior and tibialis posterior tendons, intrinsic muscles, plantar ligaments, and plantar fascia [9].

De Palma and colleagues [7] classified the ligamentous structures of the Lisfranc complex into three groups: dorsal, interosseous, and plantar. This classification was the one used in the current study. The interosseous ligaments were thicker and more prominent than the corresponding dorsal and plantar ligaments, with a more prominent low signal intensity and homogeneous appearance, except in the second and third cuneometatarsal

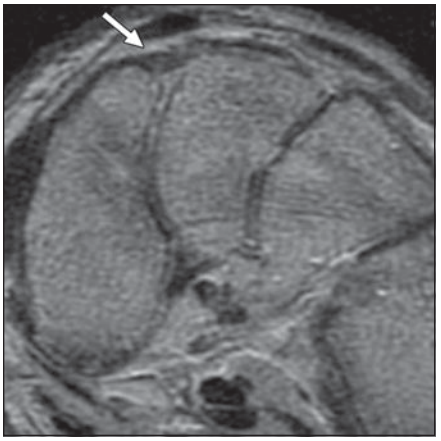

Fig. 13—Dorsal intercuneiform ligament coronal proton density MR image after injection of intraarticular gadolinium solution shows dorsal intercuneiform ligament between C1 and C2 (*arrow*).

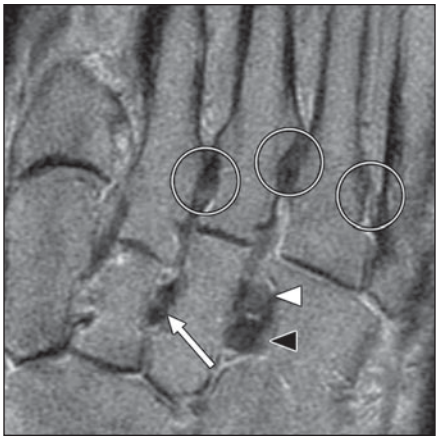

Fig. 14—Tarsal and metatarsal interosseous ligaments. Transverse oblique MR image after injection of intraarticular gadolinium solution shows intermetatarsal interosseous ligaments (*circles*), interosseus intercuneiform ligament between C2 and C3 (*arrow*) and two bands of interosseus ligament between C3 and cuboid (superior band—*white arrowhead*, inferior band—*black arrowhead*).

interosseous space. Here, they were thin (sometimes with an intricate arrangement) or even absent. The thin nature or absence of the ligaments in this region is probably explained by the solid skeletal arrangement at this level, and the strong, broad corresponding intermetatarsal and intertarsal interosseous ligaments [9, 16, 17].

There are three ligaments that connect the C1 with the base of M2, all with an oblique anterolateral orientation and located in the dorsal, interosseous, and plantar aspects of the foot [16]. The distinction between the Lisfranc and the plantar Lisfranc ligament has not always been made in previous studies [1, 6, 10, 11, 13, 15]. Potter and coworkers [14] identified the Lisfranc and the plantar ligaments as separate structures in a study of 23 patients, with injury occurring to both ligaments in three cases, only to the Lisfranc ligament in 12 cases, and only to the plantar ligament in six cases. Nevertheless, they described the plantar ligament as a discrete plantar bundle of the Lisfranc ligament, with the traditional Lisfranc ligament representing the dorsal bundle of it. We were able to identify in every specimen the plantar Lisfranc and the Lisfranc ligaments in coronal, axial, and transverse oblique images. The former ligament consisted of two bundles, one of them more superficial, inserting on the M3 base, and a deeper band attaching to the base of M2. In two specimens, these two different components did not have a common proximal insertion and originated separately from C1. This has not been described in the literature. We also became aware that the ability to discriminate the deeper band of the plantar Lisfranc from the Lisfranc ligament was only possible to some extent, as they had distinguishable borders only in their proximal portions.

The Lisfranc ligament had either a homogeneous or striated appearance, as well as low or intermediate signal intensity. The striated appearance was always associated with intermediate signal intensity. In two of the specimens, the Lisfranc ligament was found to have two bands, one superior and one inferior, which is consistent with previous descriptions [8].

In our study the length of the Lisfranc ligament was similar to that reported in the literature [7, 8], approximately 10 mm, but its thickness was greater than previously reported (7 mm versus 5 mm). This is probably because it was measured in the coronal plane, and the ligament itself is slightly oblique in orientation. Another probable reason for the discrepancy is that whenever the foot specimens had Lisfranc ligaments with two bands, these were measured together. Biomechanical evaluation of the ligamentous structures of the second TMT joint has shown that the Lisfranc ligament is stronger and stiffer than the plantar Lisfranc ligament and that the dorsal ligament is significantly weaker than the Lisfranc/plantar complex [16, 17]. This forms the rationale for nonsurgical management of the less destabilizing isolated dorsal ligament injuries.

The second and the third interosseous cuneometatarsal ligaments have a complex and variable morphology, with six possible arrangements described for the second interspace and eight types of arrangements for the third interspace [8]. Although these arrangements can be appreciated in the coronal MR images, the best planes to delineate their precise configurations are the axial and transverse oblique planes.

The intermetatarsal, intercuneiform, and C3-Cu ligaments were also identified in this study. They function as bars, reinforcing, respectively, the anterior and posterior aspect of the TMT articulation. The most lateral intermetatarsal ligament (M4-M5) is particularly important to the stability of the lateral portion of the Lisfranc joint [9]. This was confirmed by our observation of a thicker and broader interosseous ligament at this level.

In conclusion, MRI allows exquisite depiction of all the elements of the Lisfranc joint complex. An awareness of the components of this complex is a prerequisite to understanding the physiology, biomechanics, and patterns of injury of the midfoot.

References

1. Preidler KW, Brossmann J, Daenen B, Goodwin D, Schweitzer M, Resnick D. MR imaging of the tarsometatarsal joint: analysis of injuries in 11 patients. *AJR* 1996; 167:1217–1222
2. Thompson MC, Mormino MA. Injury to the tarsometatarsal joint complex. *J Am Acad Orthop Surg* 2003; 11:260–267
3. Solan MC, Moorman CT, Miyatomo RG, Jasper LE, Stephen MB. Ligamentous restraints of the second tarsometatarsal joint: a biomechanical evaluation. *Foot Ankle Int* 2001; 22:637–641
4. Nunley JA, Vertullo CJ. Classification, investigation, and management of midfoot sprains: Lisfranc injuries in the athlete. *Am J Sports Med* 2002; 30:871–878
5. Curtis MJ, Myerson M, Szura B. Tarsometatarsal joint injuries in the athlete. *Am J Sports Med* 1993; 21:497–502
6. Shapiro MS, Wascher DC, Finerman GAM. Rupture of Lisfranc's ligament in athletes. *Am J Sports Med* 1994; 22:687–691
7. De Palma L, Santucci A, Sabetta SP, Rapali S. Anatomy of the Lisfranc joint complex. *Foot Ankle Int* 1997; 18:356–364
8. Blouet JM, Rebaud C, Marquer Y, et al. Anatomy of the tarsometatarsal joint and its applications to dislocation of this articular interface. *Anat Clin* 1983; 5:9–16
9. Preidler KW, Wang YC, Brossmann J, Trudell D, Daenen B, Resnick D. Tarsometatarsal joint: anatomic details on MR images. *Radiology* 1996; 99:733–736
10. Rand T, Frank L, Pretterklieber M, Muhle C,

Resnick D. Intertarsal ligaments: high resolution MRI and anatomic correlation. *J Comput Assist Tomogr* 2000; 24:584–593

11. Delfaut EM, Rosenberg ZS, Demondion X. Malalignment at Lisfranc joint: MR features in asymptomatic patients and cadaveric specimens. *Skeletal Radiol* 2002; 31:499–504
12. Norfray JF, Geline R, Steinberg R, Galinksi A, Gilula L. Subtleties of Lisfranc fracture dislocations. *AJR* 1981; 137:1151–1156
13. Preidler KW, Peicha G, Lajtai G, et al. Conventional radiography, CT, and MR imaging in patients with hyperflexion injuries of the foot: diagnostic accuracy in the detection of bony and ligamentous changes. *AJR* 1999; 173:1673–1677
14. Potter HG, Deland JT, Gusmer PB, Carson E, Warren R. Magnetic resonance imaging of the Lisfranc ligament of the foot. *Foot Ankle Int* 1998; 19:438–446
15. Sarrafian SK. *Anatomy of the foot and ankle: descriptive, topographic, functional*, 2nd ed. Philadelphia, PA: J.B. Lippincott, 1993
16. Chiodo CP, Myerson M. Developments and advances in the diagnosis and treatment of injuries to the tarsometatarsal joint. *Orthop Clin North Am* 2001; 32:11–20
17. Kura H, Luo Z, Kitaoka HB, Smutz WP, An K. Mechanical behavior of Lisfranc and dorsal cuneometatarsal ligaments: in vitro biomechanical study. *J Orthop Trauma* 2001; 15:107–110